Article

Cell Reports

GDH-Dependent Glutamate Oxidation in the Brain Dictates Peripheral Energy Substrate Distribution

Graphical Abstract

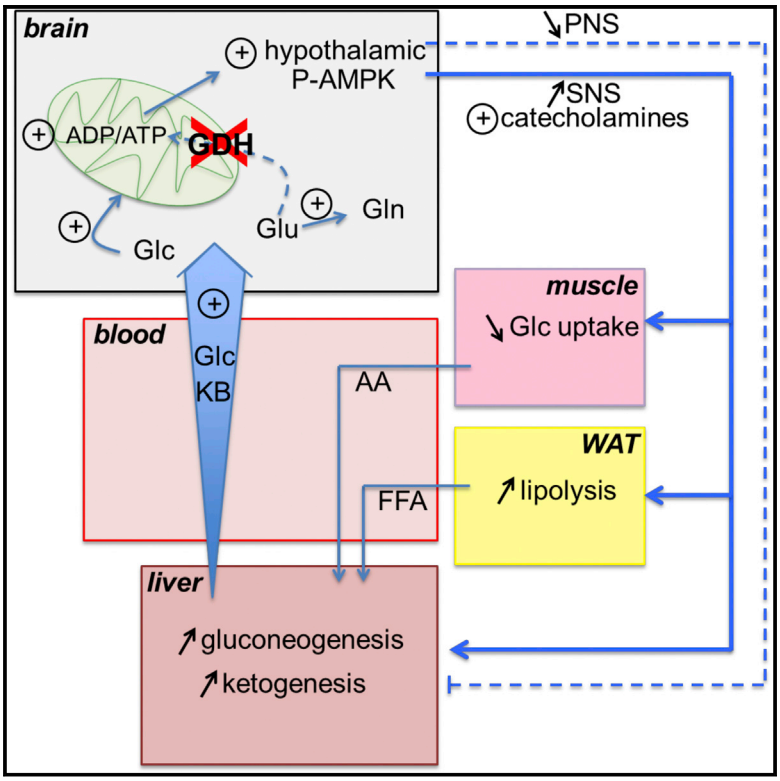

Highlights

- Glutamate is an energy substrate through GDH activity in the brain
- Central GDH deficit increases hypothalamic ADP/ATP ratios and activates AMPK
- Lack of glutamate utilization is compensated by increased brain glucose usage
- Lack of central glutamate consumption reshapes energy stores in periphery

Authors

Melis Karaca, Francesca Frigerio, Stephanie Migrenne, ..., Helle S. Waagepetersen, Christophe Magnan, Pierre Maechler

Correspondence

pierre.maechler@unige.ch

In Brief

The neurotransmitter glutamate is released by neurons and recycled by astrocytes in the brain. Karaca at al. disrupt CNS oxidative metabolism of glutamate, resulting in increased brain glucose consumption and mobilization of energy substrates from the periphery through the autonomous nervous system, thus showing that glutamate participates in central energy provision.

Karaca et al., 2015, Cell Reports *13*, 1–11
October 13, 2015 ©2015 The Authors
http://dx.doi.org/10.1016/j.celrep.2015.09.003

CellPress

Please cite this article in press as: Karaca et al., GDH-Dependent Glutamate Oxidation in the Brain Dictates Peripheral Energy Substrate Distribution, Cell Reports (2015), http://dx.doi.org/10.1016/j.celrep.2015.09.003

Cell Reports
Article

GDH-Dependent Glutamate Oxidation in the Brain Dictates Peripheral Energy Substrate Distribution

Melis Karaca,[1] Francesca Frigerio,[1] Stephanie Migrenne,[2] Juliette Martin-Levilain,[1] Dorte M. Skytt,[3] Kamilla Pajecka,[3] Rafael Martin-del-Rio,[4] Rolf Gruetter,[5] Jorge Tamarit-Rodriguez,[4] Helle S. Waagepetersen,[3] Christophe Magnan,[2] and Pierre Maechler[1,*]

[1]Department of Cell Physiology and Metabolism, CMU, University of Geneva, rue Michel Servet 1, 1205 Geneva, Switzerland
[2]CNRS, BFA, University Paris Diderot, 4 rue Marie Andrée Lagroua Weill-Halle, 75205 Paris Cedex 13, France
[3]Department of Drug Design and Pharmacotherapy, Faculty of Health and Medical Sciences, University of Copenhagen, 2 Universitetsparken, 2100 Copenhagen, Denmark
[4]Department of Biochemistry, Medical School, Complutense University, 28040 Madrid, Spain
[5]LIFMET, CIBM, Ecole Polytechnique Fédérale de Lausanne, 1015 Lausanne, Switzerland
*Correspondence: pierre.maechler@unige.ch
http://dx.doi.org/10.1016/j.celrep.2015.09.003

SUMMARY

Glucose, the main energy substrate used in the CNS, is continuously supplied by the periphery. Glutamate, the major excitatory neurotransmitter, is foreseen as a complementary energy contributor in the brain. In particular, astrocytes actively take up glutamate and may use it through oxidative glutamate dehydrogenase (GDH) activity. Here, we investigated the significance of glutamate as energy substrate for the brain. Upon glutamate exposure, astrocytes generated ATP in a GDH-dependent way. The observed lack of glutamate oxidation in brain-specific GDH null Cns*Glud1*$^{-/-}$ mice resulted in a central energy-deprivation state with increased ADP/ATP ratios and phospho-AMPK in the hypothalamus. This induced changes in the autonomous nervous system balance, with increased sympathetic activity promoting hepatic glucose production and mobilization of substrates reshaping peripheral energy stores. Our data reveal the importance of glutamate as necessary energy substrate for the brain and the role of central GDH in the regulation of whole-body energy homeostasis.

INTRODUCTION

In the CNS, the role of glutamate as a signaling molecule for excitatory transmission acting through neuronal receptors is well described (Baudry and Lynch, 1979). Furthermore, glutamate is a key metabolite for both nitrogen and energy metabolism in the brain (Escartin et al., 2006). Disturbances in central glutamate homeostasis are associated with neurological disorders such as schizophrenia and epilepsy (Gaisler-Salomon et al., 2009; Gordon, 2010; Harris et al., 2009; Meldrum, 1994). Upon glutamatergic transmission, intersynaptic glutamate clearance is achieved mostly by glial cells, namely astrocytes (Bak et al., 2006). Such active uptake prevents glutamate accumulation in the extracellular space and associated toxicity. Following its uptake, glutamate may be amidated to glutamine and then recycled back to neurons (i.e., the glutamate-glutamine cycle). Alternatively, glutamate may be used by astrocytes as an energy substrate via deamination to α-ketoglutarate before further oxidation in the tricarboxylic acid (TCA) cycle, thereby promoting ATP generation (McKenna et al., 1996; Yu et al., 1982). In vitro, glutamate has been shown to be oxidized in a variety of different brain tissue preparations (Zielke et al., 2009). In vivo, the contribution of glutamate as a metabolic substrate for energy production within the brain is still uncertain (Magistretti et al., 1999; Peters et al., 2004; Zielke et al., 2009).

Because of substrate selectivity across the blood-brain barrier, glucose is the main energy source delivered by the periphery to the CNS (Vannucci et al., 1997), and astrocytes phosphorylate approximately half of this plasma-derived glucose (Nehlig, 2004). Subsequent to its phosphorylation, glucose is metabolized through glycolysis, and then glucose carbons may follow pathways other than the TCA cycle (Verleysdonk and Hamprecht, 2000). In addition, glucose is an important modulator of central regulation of the peripheral energy balance. Specific hypothalamic and brainstem neurons increase their firing rate in response to high or low glucose concentrations (Karnani and Burdakov, 2011; Yang et al., 2004). Current models propose that hypothalamic nutrient-sensing mechanisms regulate food intake, hormonal responses, and hepatic glucose production in order to maintain energy homeostasis (Blouet and Schwartz, 2010; Lam et al., 2009).

In the brain, glutamate is predominantly derived from glucose catabolism and subsequent TCA cycle metabolism (Gruetter et al., 1994; Hertz et al., 2007). The latter provides substrates for glutamate dehydrogenase (GDH), an essential enzyme connecting glucose and glutamate metabolism (Karaca et al., 2011). This mitochondrial enzyme catalyzes the reversible reaction α-ketoglutarate + NH_3 + NADH ↔ glutamate + NAD^+ (Sanner, 1975). GDH is a homohexamer (Hucho et al., 1975) encoded by the well-conserved 45-kb *GLUD1* gene (Michaelidis et al.,

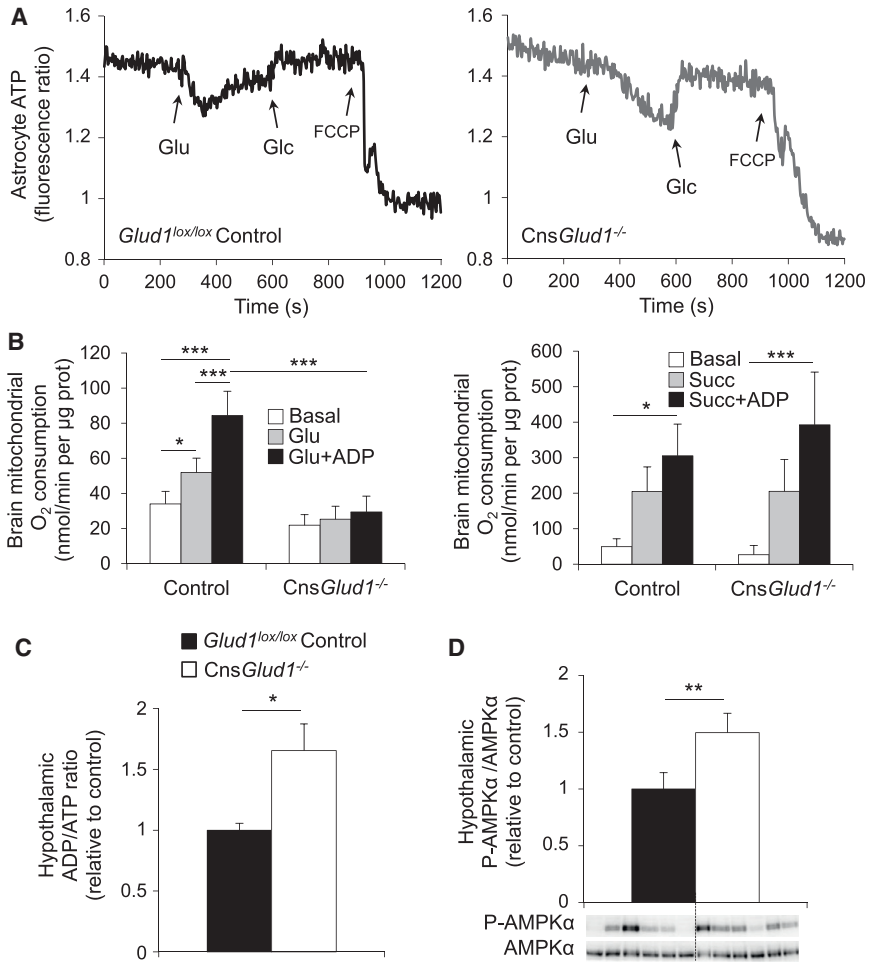

Figure 1. Lack of GDH in Cns*Glud1*$^{-/-}$ Brains Impairs Glutamate-Induced Energy Generation

(A) Representative recordings of cellular ATP in control *Glud1*$^{lox/lox}$ (left panel) and GDH null Cns*Glud1*$^{-/-}$ isolated astrocytes (right panel) expressing the FRET-based ATP indicator. Cultured astrocytes were stimulated with 500 µM glutamate (Glu) followed by 6 mM glucose (Glc) before mitochondrial uncoupling with 1 µM FCCP.

(B) Oxygen consumption in mitochondria isolated from *Glud1*$^{lox/lox}$ control and Cns*Glud1*$^{-/-}$ brains in response to 10 mM glutamate (Glu) (left panel) and 5 mM succinate (Succ) (right panel) in the presence or absence of 100 µM ADP (n = 5). See also Figure S1.

(C) Hypothalamic ADP/ATP ratio from *Glud1*$^{lox/lox}$ control and Cns*Glud1*$^{-/-}$ mice (n = 4–5).

(D) Immunoblotting on hypothalamic extracts from *Glud1*$^{lox/lox}$ control and Cns*Glud1*$^{-/-}$ mice showing phospho-AMPKα (P-AMPKα) relative to total AMPKα levels (n = 6).

All values are means ± SEM. *p < 0.05; **p < 0.01; ***p < 0.001.

RESULTS

Brain-Specific Deletion of GDH Leads to Central Energy Deficiency

Brain-specific GDH knockout (Cns*Glud1*$^{-/-}$) mice were generated by crossing *Glud1*$^{lox/lox}$ with Nestin-*Cre* mice (Frigerio et al., 2012). We previously reported that the lack of GDH in the CNS modifies the metabolic fate of glutamate without altering synaptic transmission in basal conditions (Frigerio et al., 2012).

Glutamate may be catabolized by GDH through oxidative deamination fueling the TCA cycle and, as a consequence, activation of the respiratory chain potentially generating ATP. In order to characterize GDH-dependent energy substrates of the CNS, cellular ATP was measured in response to glutamate and glucose. When *Glud1*$^{lox/lox}$ control astrocytes were stimulated with glutamate, ATP levels were transiently lowered for ~1 min, possibly due to energy-consuming glutamate uptake (Danbolt, 2001; McKenna, 2013), before sustained ATP elevation (Figure 1A). In GDH null Cns*Glud1*$^{-/-}$ astrocytes, ATP levels failed to increase in response to glutamate, as only a continuous drop was observed (Figure 1A). However, both *Glud1*$^{lox/lox}$ control and Cns*Glud1*$^{-/-}$ astrocytes were responsive to glucose stimulation (Figure 1A). Oxygen consumption was induced in control brain mitochondria upon glutamate stimulation and was further enhanced by the addition of ADP (Figure 1B). On the contrary, glutamate did not increase respiration of Cns*Glud1*$^{-/-}$ brain mitochondria (Figure 1B). In order to test GDH-independent mitochondrial respiration, succinate was used as a substrate and induced similar oxygen consumption in control and Cns*Glud1*$^{-/-}$ brain mitochondria (Figure 1B). As an additional

1993). In the CNS, GDH is predominantly expressed in astrocytes (Mastorodemos et al., 2005), an alternative pathway to glutamate-glutamine cycling that provides neurotransmitter precursors for glutamatergic neurons. Related to the high capacity for glutamate uptake by astrocytes, GDH is a putative regulator of brain energy homeostasis through the glutamate oxidative pathway.

The present study investigated the role of GDH in the selectivity of energy substrates within the CNS, in particular the recycling of the neurotransmitter glutamate versus glucose provided by the periphery. Analysis of brain-specific GDH null Cns*Glud1*$^{-/-}$ mice revealed a major impact on peripheral energy partitioning compatible with the "selfish brain" paradigm (Peters et al., 2004). According to this model, the brain may reroute energy substrates at the expense of peripheral tissues whenever necessary. The lack of GDH-dependent glutamate oxidation in Cns*Glud1*$^{-/-}$ brains established an energy-deprivation state despite normoglycemia. This induced changes in the autonomous nervous system balance, favoring the mobilization of glucose and ketone bodies from the periphery through AMPK-dependent mechanisms. This study reveals the role of central GDH in the regulation of whole-body energy homeostasis.

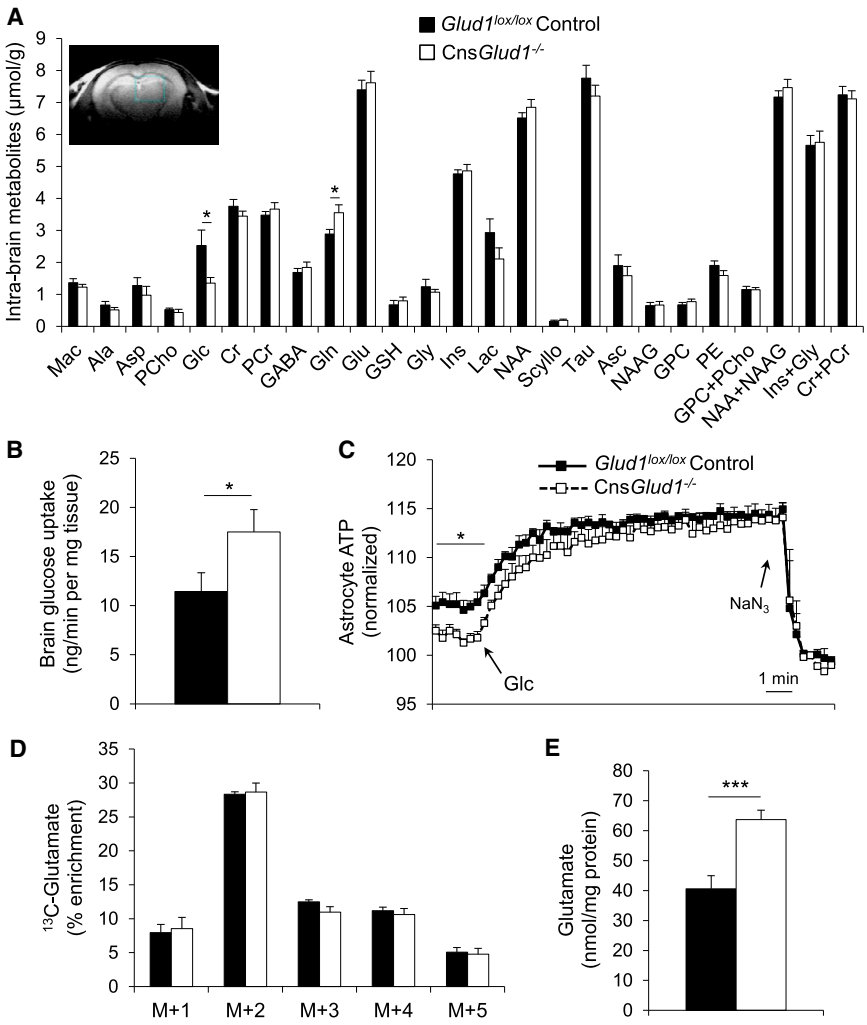

Figure 2. Lack of GDH in Cns*Glud1*$^{-/-}$ Brains Increases Glucose Utilization

(A) Intra-brain metabolite concentrations measured by NMR (^{1}H-MRS) on living *Glud1*$^{lox/lox}$ control and Cns*Glud1*$^{-/-}$ mice (n = 9–10). The blue square on the slice image represents the volume of interest that was analyzed; Mac, macromolecules; Ala, alanine; Asp, aspartate; PCho, phosphorylcholine; Glc, glucose; Cr, creatine; PCr, phosphocreatine; GABA, γ-aminobutyric acid; Gln, glutamine; Glu, glutamate; GSH, glutathion; Gly, glycine; Ins, myo-inositol; Lac, lactate; NAA, N-acetylaspartate; Scyllo, scyllo inositol; Tau, taurine; Asc, ascorbate; NAAG, N-acetylaspartylglutamate; GPC, glycerophosphocholine; and PE, phosphoethanolamine.

(B) Brain glucose uptake of *Glud1*$^{lox/lox}$ control and Cns*Glud1*$^{-/-}$ mice following intravenous [^{14}C]-2-deoxyglucose ([^{14}C]-2-DG) administration (n = 5–6).

(C) Cellular ATP levels of *Glud1*$^{lox/lox}$ control and Cns*Glud1*$^{-/-}$ astrocytes expressing luciferase-based ATP reporter. Cultured astrocytes were stimulated with 6 mM glucose (Glc) before mitochondrial poisoning with 2 mM NaN_3 (n = 9). Values are normalized to basal levels without mitochondrial contribution (+NaN_3).

(D and E) ^{13}C-glutamate percent enrichment (D) and total amount (nmol/mg protein) (E) obtained from [U-^{13}C]glucose incubation of astrocytes isolated from *Glud1*$^{lox/lox}$ control and Cns*Glud1*$^{-/-}$ mice (n = 5–7).

All values are means ± SEM. *p < 0.05; ***p < 0.001.

control of tissue specificity, we analyzed mitochondria isolated from liver, notably rich in GDH. Liver GDH activity was comparable between *Glud1*$^{lox/lox}$ control and Cns*Glud1*$^{-/-}$ mice, and respiration was similarly induced by glutamate and succinate in Cns*Glud1*$^{-/-}$ liver mitochondria compared to controls (Figures S1A and S1B). These data show that astrocytes can generate ATP upon glutamate stimulation in a GDH-dependent manner.

In the absence of GDH-dependent glutamate oxidation, Cns*Glud1*$^{-/-}$ animals showed increased hypothalamic ADP to ATP ratio (+65%, p < 0.05; Figure 1C). This correlated with increased hypothalamic levels of phospho-AMPK (P-AMPK) (+50%, p < 0.01), a major sensor of cellular energy deprivation (Figure 1D).

As revealed by nuclear magnetic resonance (NMR) measurements in living non-fasted animals (Figure 2A), intra-brain glutamine concentrations were higher in knockout mice than control mice (+23%, p < 0.05), in accordance with impaired glutamate consumption (Frigerio et al., 2012). Conversely, brain glucose concentrations were lower in Cns*Glud1*$^{-/-}$ mice than controls (−47%, p < 0.05) in conditions of peripheral normoglycemia (Figures 2A). Of note, the lower brain glucose observed in knockout mice remained in the range associated with peripheral euglycemia (i.e., brain glucose 0.8–2.6 µmol/g and plasma glucose 4.5–10 mM; Choi et al., 2001). Glucose uptake was higher in Cns*Glud1*$^{-/-}$ brains than in controls (+54%, p < 0.05; Figures 2B). Astrocyte cultures isolated from Cns*Glud1*$^{-/-}$ animals had slightly lower basal ATP levels when glucose deprived. However, they robustly generated ATP upon glucose stimulation, exhibiting compensatory glucose response compared with controls (Figure 2C). The increased glucose consumption in the brain of Cns*Glud1*$^{-/-}$ mice was further evidenced by an increased incorporation of ^{13}C from ^{13}C-glucose into the glutamate pool. The ^{13}C enrichment was maintained, although the total cellular content of glutamate (nmol/mg protein) was elevated by 50% (Figures 2D and 2E). The ^{13}C-labeling of glutamate reflects glucose metabolism (i.e., acetyl-coenzyme A enrichment and TCA cycle metabolism) due to the high activity of aspartate aminotransferase (Mason et al., 1995). Altogether, these data show central glutamate-dependent energy deficit in Cns*Glud1*$^{-/-}$ mice, compensated by increased glucose usage in the brain.

Lack of Brain GDH Reshapes Body Composition and Alters Peripheral Glucose Homeostasis

Brain energy homeostasis is modulated by the cross-talks between CNS and metabolically active peripheral tissues. However, it primarily relies on the provision of exploitable substrates

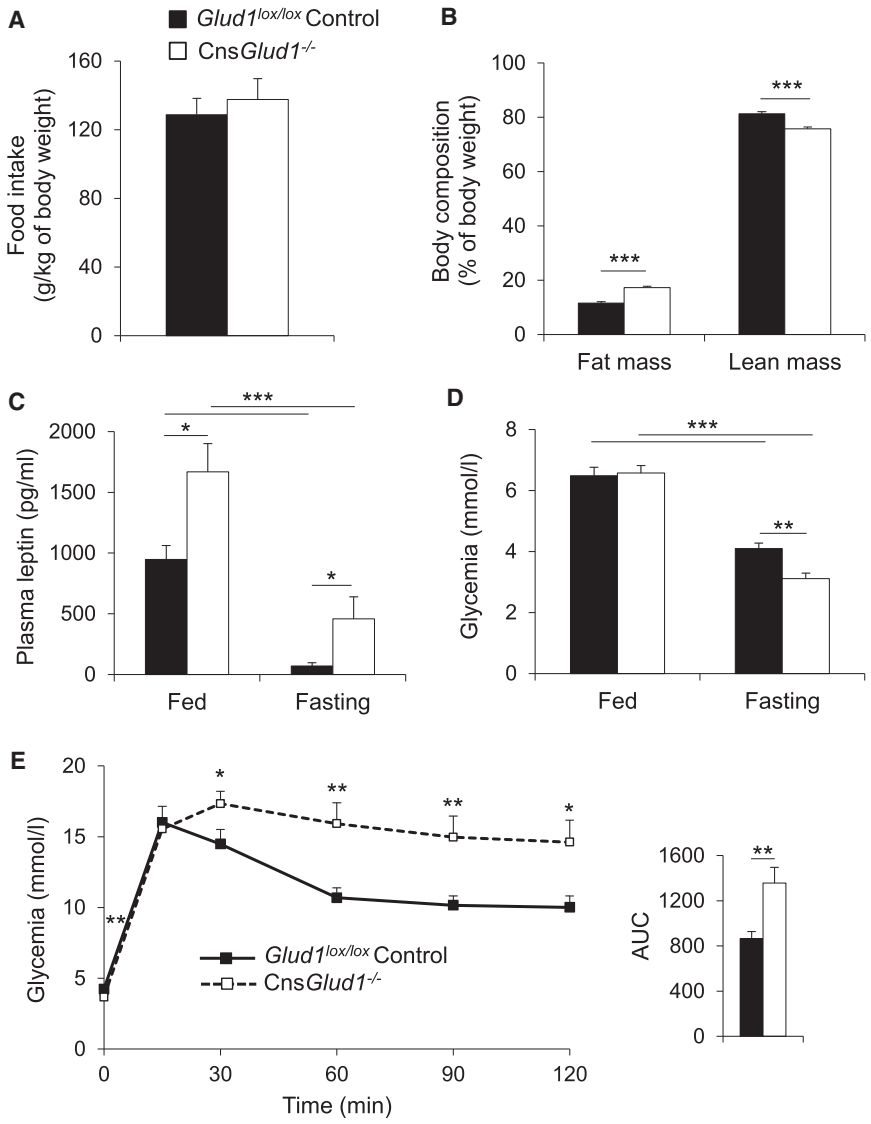

Figure 3. Lack of GDH in CnsGlud1$^{-/-}$ Brains Modifies Lean/Fat Mass Distribution and Alters Glucose Homeostasis

(A) Food intake recorded over a representative 24-hr period. See also Figure S2.

(B) Body composition showing lean and fat mass distribution in *Glud1*$^{lox/lox}$ Control and CnsGlud1$^{-/-}$ mice measured by EchoMRI (n = 17–20). See also Figure S3.

(C) Plasma leptin levels in fed and overnight-fasting *Glud1*$^{lox/lox}$ control and CnsGlud1$^{-/-}$ mice (n = 7).

(D) Plasma glucose levels in fed and overnight-fasting *Glud1*$^{lox/lox}$ control and CnsGlud1$^{-/-}$ mice (n = 9–10). See also Figure S3.

(E) Glucose tolerance test (1 g/kg) in *Glud1*$^{lox/lox}$ control and CnsGlud1$^{-/-}$ mice (left panel) and its quantification as AUC (right panel) (n = 12–13). AUC, area under the curve.

All values are means ± SEM. *p < 0.05; **p < 0.01; ***p < 0.001.

delivered from the periphery, which is influenced by the balance of food intake and energy expenditure. CnsGlud1$^{-/-}$ mice did not modify their feeding behavior to compensate for the loss of central glutamate-derived energy (Figures 3A and S2A). However, as assessed by quantitative magnetic resonance (Figure 3B), their body composition was reshaped with increased fat mass (+50%, $p < 0.001$) and decreased lean mass (−7%, $p < 0.001$), without affecting total body weight. Increased plasma leptin levels in CnsGlud1$^{-/-}$ animals, reflecting the extent of fat depots, paralleled adipose tissue mass (Figure 3C). Although we observed lower spontaneous locomotor activity during the daytime in CnsGlud1$^{-/-}$ mice (Figure S2B), the VO_2 and VCO_2 were not significantly different compared to control mice (Figures S2C and S2D). The calculated VCO_2/VO_2 revealed no difference in respiratory exchange ratio (RER) between the two groups (Figures S2E and S2F). Finally, body heat production and water intake were similar in CnsGlud1$^{-/-}$ mice and controls (Figures S2G and S2H). Therefore, analyzed at the whole-body level, CnsGlud1$^{-/-}$ mice exhibited comparable metabolic rates with similar proportions of carbohydrate versus fatty acid oxidation. Normalization of parameters from metabolic cages (Figure S2) to lean mass (Figure 3B) resulted in similar outcome (data not shown). These data demonstrate that ablation of GDH in the brain modified energy distribution in the periphery without affecting food intake and overall energy expenditure.

Glucose is the main energy substrate contributed by the periphery to the CNS. The elevated glucose usage in CnsGlud1$^{-/-}$ brain prompted us to investigate peripheral glucose homeostasis. Although the glycemia was unchanged under fed conditions, fasting CnsGlud1$^{-/-}$ mice had lower blood glucose levels than *Glud1*$^{lox/lox}$ controls (−22%, $p < 0.01$) (Figure 3D). Glucose tolerance tests revealed impaired glucose clearance in CnsGlud1$^{-/-}$ animals with an area under the curve (AUC) increased by 57% ($p < 0.01$) (Figure 3E). These data show that central energy perturbation in CnsGlud1$^{-/-}$ mice impairs peripheral glucose homeostasis.

Nestin-*Cre* Transgene Does Not Contribute to the Metabolic Phenotype of CnsGlud1$^{-/-}$ Mice

To rule out the possibility that the Nestin-*Cre* transgene used in the study may have independently contributed to the metabolic phenotype, we analyzed in parallel transgenic mice carrying only the Nestin-*Cre* transgene and their respective Nestin-*Cre*-negative littermates. We previously reported that CnsGlud1$^{-/-}$ mice express normal levels of GDH in non-brain tissues such as liver, kidney, or spleen (Karaca and Maechler, 2014). Additionally, no differences in body weight (Figure S3A; Karaca and Maechler, 2014), body composition (Figure S3B), and glycemia (Figure S3C)

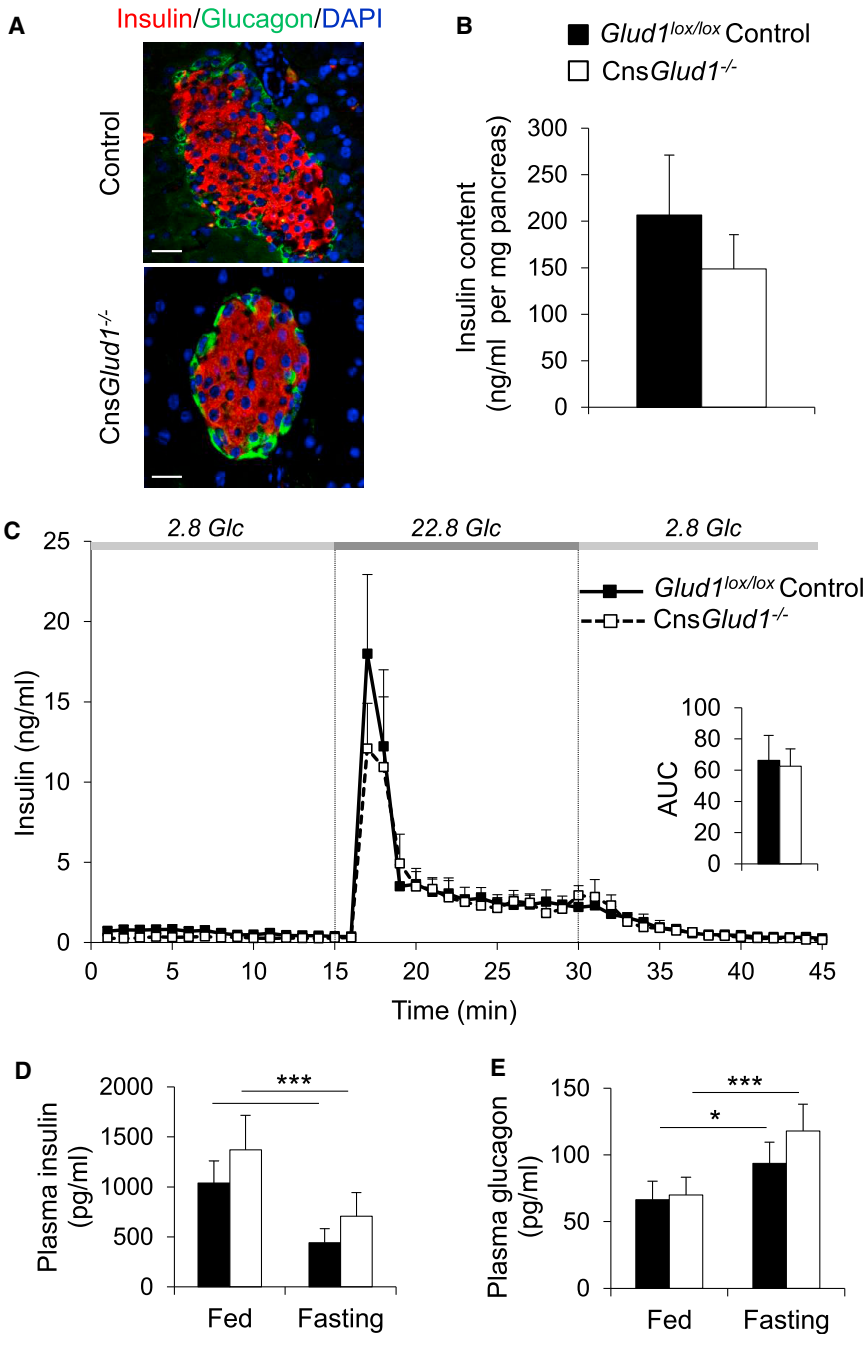

Figure 4. Function of Pancreatic Islet Is Preserved in Cns*Glud1*$^{-/-}$ Mice

(A) Representative images of immunohistochemical analyses on pancreas sections from *Glud1*$^{lox/lox}$ control and Cns*Glud1*$^{-/-}$ mice co-stained for insulin (red), glucagon (green), and nuclei (blue). Scale bar, 20 μm.

(B) Insulin contents of pancreata isolated from *Glud1*$^{lox/lox}$ Control and Cns*Glud1*$^{-/-}$ mice (n = 5).

(C) Glucose-stimulated insulin release determined using in situ pancreatic perfusions on *Glud1*$^{lox/lox}$ control and Cns*Glud1*$^{-/-}$ mice. Glucose was raised from basal 2.8 mM (2.8 Glc) to stimulatory 22.8 mM (22.8 Glc) (left panel). The insulin secreted over the stimulatory period is presented as AUC (right panel) (n = 4–8). AUC, area under the curve. See also Figure S4.

(D and E) Plasma insulin (D, n = 10) and glucagon (E, n = 17–22) levels in fed and overnight fasting *Glud1*$^{lox/lox}$ Control and Cns*Glud1*$^{-/-}$ mice. See also Figure S4.

All values are means ± SEM. *p < 0.05; ***p < 0.001.

were observed between genotypes, being either Nestin-*Cre* negative or Nestin-*Cre* positive. Accordingly, Nestin-*Cre* transgene did not contribute to the metabolic phenotype observed in Cns*Glud1*$^{-/-}$ mice, supporting the use of *Glud1*$^{lox/lox}$ littermates as a control group, which allows homogenization of the genetic background.

Pancreatic Islet Function Is Preserved in Cns*Glud1*$^{-/-}$ Mice

Inability to properly regulate glycemia after a glucose load could be due to altered pancreatic function. Immunohistochemistry performed on pancreas sections showed normal islet architecture when co-stained for insulin and glucagon (Figure 4A). Pancreatic insulin content was similar between *Glud1*$^{lox/lox}$ control and Cns*Glud1*$^{-/-}$ mice (Figure 4B). We performed in situ pancreatic perfusions to test the β cell response in islets maintained in their native pancreatic environment. This revealed normal glucose-stimulated insulin secretion when pancreas of Cns*Glud1*$^{-/-}$ were compared with those of *Glud1*$^{lox/lox}$ controls (Figure 4C). A similar profile was observed with in vitro perifusion of isolated islets stimulated with 22.8 mM glucose (Figure S4A). Finally, circulating insulin, C-peptide, and glucagon levels did not differ between Cns*Glud1*$^{-/-}$ and *Glud1*$^{lox/lox}$ controls, either in fed or fasting conditions (Figures 4D, 4E, and S4B). These data show that the defect in glucose homeostasis in Cns*Glud1*$^{-/-}$ mice is not contributed by an altered pancreatic function.

Hepatic Glucose Production Is Increased in Cns*Glud1*$^{-/-}$ Mice

Besides the β cell, altered glucose homeostasis could result from increased endogenous glucose production and/or decreased glucose uptake by peripheral tissues, in particular muscles and adipocytes. The glucose turnover rate was assessed using the hyperinsulinemic-euglycemic clamp technique. The whole-body glucose utilization rate (GUR) was not different between

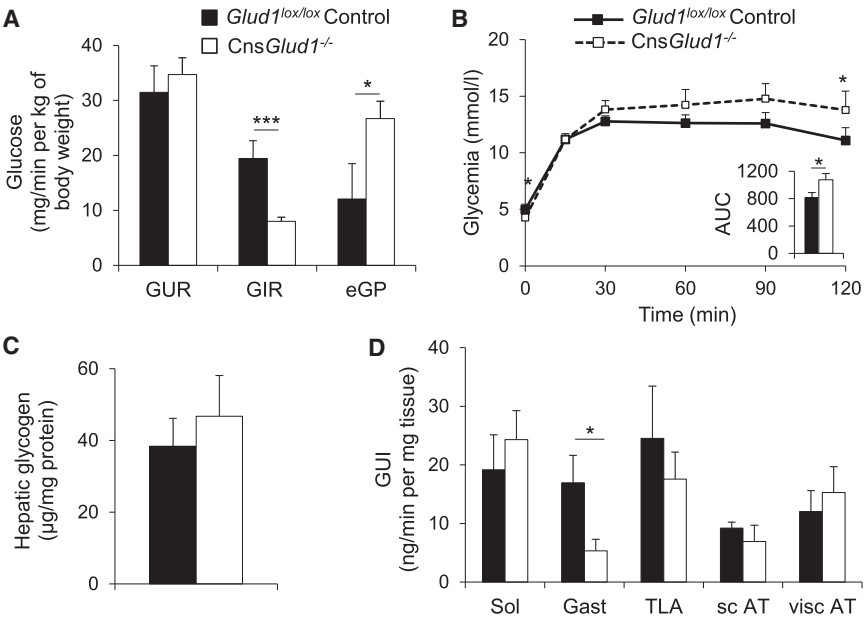

Figure 5. Hepatic Glucose Production Is Enhanced in Cns*Glud1*$^{-/-}$ Mice

(A) Glucose turnover rate determined by hyperinsulinemic-euglycemic clamp experiments on *Glud1*$^{lox/lox}$ control and Cns*Glud1*$^{-/-}$ mice (n = 7–13). Glucose utilization rate (GUR), glucose infusion rate (GIR), and endogenous glucose production (eGP) are shown here.

(B) Hepatic glucose production assessed by pyruvate challenge (2 g/kg) in *Glud1*$^{lox/lox}$ control and Cns*Glud1*$^{-/-}$ mice and blood glucose quantification by the AUC (n = 11). AUC, area under the curve.

(C) Hepatic glycogen contents measured in livers collected from non-fasted *Glud1*$^{lox/lox}$ control and Cns*Glud1*$^{-/-}$ mice (n = 7).

(D) Glucose utilization index (GUI) in soleus (Sol), gastrocnemius (Gast), and tibialis anterior (TLA) muscles, as well as in subcutaneous (sc) and visceral (visc) adipose tissues (AT). Measurements are from clamp experiments on *Glud1*$^{lox/lox}$ control and Cns*Glud1*$^{-/-}$ mice upon injection of [^{14}C]-2-deoxyglucose (n = 6–11).

All values are means ± SEM. *p < 0.05; ***p < 0.001.

Glud1$^{lox/lox}$ control and Cns*Glud1*$^{-/-}$ mice (Figure 5A), although less glucose was needed to maintain euglycemia, as shown by the decreased glucose infusion rate (GIR) (−59%, p < 0.001, Figure 5A). This observation correlated with increased endogenous glucose production (eGP) (+121%, p < 0.05) in Cns*Glud1*$^{-/-}$ mice when compared with *Glud1*$^{lox/lox}$ controls (Figure 5A). Glucose derived from pyruvate reflects hepatic gluconeogenesis. A pyruvate challenge induced higher blood glucose levels in Cns*Glud1*$^{-/-}$ mice than in *Glud1*$^{lox/lox}$ controls (Figure 5B). Hepatic glycogen concentrations measured both under fed (Figure 5C) and fasting (not shown) conditions were similar between groups, indicating that glycogenolysis did not account for the observed higher glucose production. Measurements of 2-deoxyglucose uptake during the hyperinsulinemic clamp revealed lower uptake in mixed gastrocnemius muscle (−69%, p < 0.05), while there was no difference in the soleus and tibialis anterior muscles or subcutaneous and visceral adipose tissues (Figure 5D). These data show that the increased glucose availability in Cns*Glud1*$^{-/-}$ mice was due to higher liver gluconeogenesis and lower muscle glucose uptake.

Energy Substrates Are Mobilized from Peripheral Tissues in Cns*Glud1*$^{-/-}$ Mice

In conditions of energy scarcity in the CNS, amino acids can be mobilized from skeletal muscles for hepatic gluconeogenesis (glucogenic amino acids: Asp, Glu, Ser, Gln, His, Gly Thr, Arg, Ala, Val, Tyr, Phe, and Ile) and ketogenesis (ketogenic amino acids: Leu, Tyr, Phe, and Ile). Plasma concentrations of most amino acids were markedly reduced in both fed and fasting conditions in Cns*Glud1*$^{-/-}$ mice in comparison with *Glud1*$^{lox/lox}$ control mice, in particular the ketogenic ones (Figure 6A). Accordingly, circulating ketone bodies, in particular β-hydroxybutyrate, were higher in Cns*Glud1*$^{-/-}$ mice (+49%, p < 0.01; Figure 6B). Regarding plasma lipids in Cns*Glud1*$^{-/-}$ mice, both free fatty acids (+36%, p < 0.01) and triglycerides (+56%, p < 0.001) were elevated in comparison with *Glud1*$^{lox/lox}$ controls (Figures 6C and 6D). Upon energy need, lipolysis of fat stored as triglycerides in adipose tissues releases free fatty acids used for β-oxidation, ketogenesis, and reformation of triglyceride-rich lipoproteins in the liver. Higher expression of hormone sensitive lipase (HSL) in adipose tissue of Cns*Glud1*$^{-/-}$ mice further confirmed enhanced lipid turnover in brain GDH null animals (Figure 6E). These data show that mobilization of energy substrates from peripheral tissues is increased in Cns*Glud1*$^{-/-}$ mice.

Substrate Mobilization in Cns*Glud1*$^{-/-}$ Mice Is Orchestrated by the Autonomous Nervous System

Next, hormones responsible for substrates mobilization were analyzed. Plasma concentrations of corticosterone as well as those of the pancreatic hormone glucagon remained unchanged in Cns*Glud1*$^{-/-}$ and *Glud1*$^{lox/lox}$ control mice (Figures 7A and 4E). Remarkably, Cns*Glud1*$^{-/-}$ mice exhibited an increase in catecholamine levels (epinephrine, +36%, p < 0.05; norepinephrine, +42%, p < 0.05) along with a decrease in plasma pancreatic polypeptide levels (−63%, p < 0.05) compared with *Glud1*$^{lox/lox}$ controls (Figures 7B–7D). Catecholamines are stimulated by the sympathetic nervous system (SNS), while pancreatic polypeptide is commonly used as a marker of parasympathetic activity. Higher global SNS activity in Cns*Glud1*$^{-/-}$ mice was uncovered by in vivo nerve recordings, performed in non-fasted normoglycemic conditions, showing increased firing rates of the sympathetic nerve compared to controls (Figures 7E and 7F). To directly test whether SNS outflow onto liver was affected in Cns*Glud1*$^{-/-}$ mice, we used the synthesis inhibition method (Brodie et al., 1966) in order to measure the catecholamine turnover rate (TR). In the liver of Cns*Glud1*$^{-/-}$ mice, there was a 1.8-fold increase in basal norepinephrine (NE) concentrations [NE_0] compared to controls. The fractional turnover constant *k* was

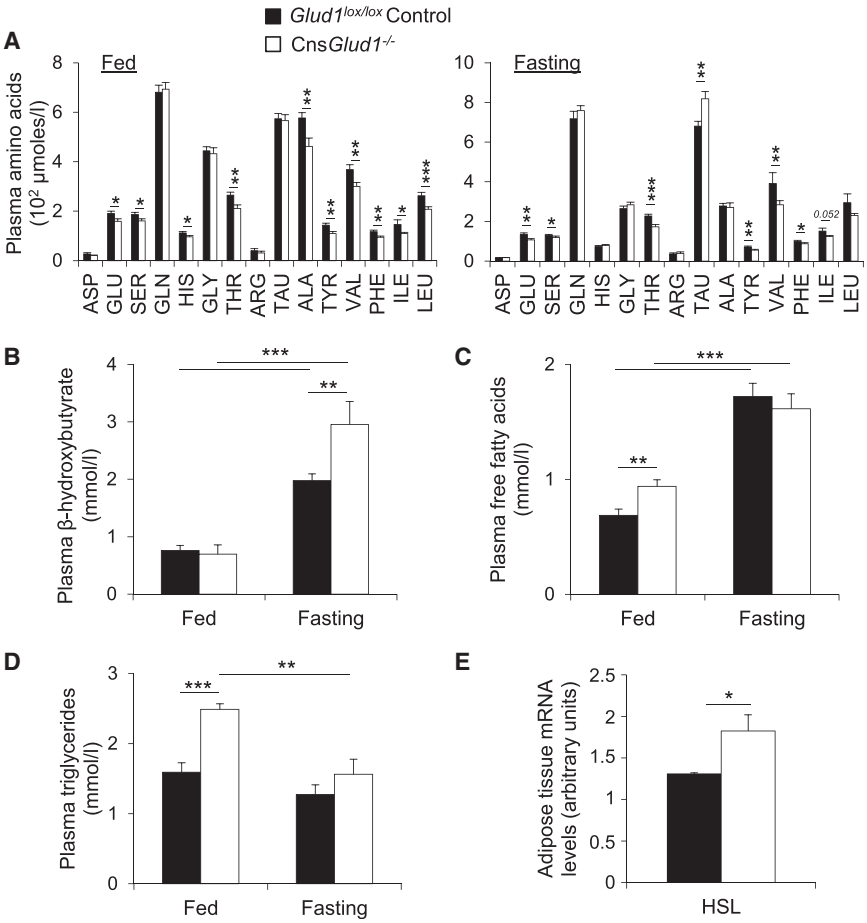

Figure 6. Increased Peripheral Mobilization of Energy Substrates in CnsGlud1$^{-/-}$ Mice

(A) Concentrations of circulating amino acids in fed (left panel) and overnight fasting (right panel) *Glud1*$^{lox/lox}$ control and CnsGlud1$^{-/-}$ mice measured by high-performance liquid chromatography (n = 16–17).

(B–D) Plasma concentrations of β-hydroxybutyrate (B), free fatty acids (C), and triglycerides (D) in fed and overnight-fasting *Glud1*$^{lox/lox}$ control and CnsGlud1$^{-/-}$ mice (n = 6–9).

(E) Gene expression of adipose tissue hormone-sensitive lipase (HSL), normalized to cyclophilin (n = 4).

All values are means ± SEM. *p < 0.05; **p < 0.01; ***p < 0.001.

2.5-fold higher in CnsGlud1$^{-/-}$ liver, revealing a net decrease in NE half-life. TR, a readout of SNS outflow, was 4-fold higher in CnsGlud1$^{-/-}$ mice compared with controls (Figures 7G–7I).

Analysis of mice lacking brain GDH reveals that glutamate-related central energy deficiency (Figure 1) induces an increased sympathetic-to-parasympathetic balance, promoting substrate mobilization from the periphery through the liver (Figure 7).

DISCUSSION

Body energy homeostasis is controlled by complex interactions between the CNS and peripheral tissues. Although the brain represents 2% of the body's weight, it accounts for ~20% of basal energy expenditure (Kety, 1957; Rolfe and Brown, 1997; Sokoloff, 1960), requiring accurate regulation of substrate supply in order to ensure its function in various nutritional or pathological conditions.

Glucose is the essential metabolic fuel for the CNS under physiological conditions. The brain is highly dependent on a continuous glucose supply from the periphery because of its poor capacity to synthesize glucose or store glycogen. In addition, concentrations of possible alternative substrates are low under physiological conditions (e.g., ketone bodies) or their transport across the blood-brain barrier is limited (e.g., free fatty acids), thereby minimizing their use in standard conditions.

Glutamate is the most abundant excitatory neurotransmitter and, besides glucose, may also contribute to sustain brain energy homeostasis. Accordingly, glutamate can be oxidized by astrocytes at higher rate than glucose, 3-hydroxybutyrate, glutamine, lactate, or malate (McKenna, 2012). Following its uptake by astrocytes, the glutamate fraction escaping the glutamate-glutamine cycle can be converted to α-ketoglutarate, either by transamination reactions or by NADH-producing oxidation catalyzed by GDH, an enzyme abundant in astrocytes (Lovatt et al., 2007; McKenna, 2007; Zaganas et al., 2001, 2012). The oxidative catabolism of glutamate proceeds primarily via GDH in rat astrocytes (McKenna et al., 1996; Westergaard et al., 1996). The α-ketoglutarate derived from glutamate activates the TCA cycle, thereby promoting ATP production by the respiratory chain. According to these pathways, GDH might play a pivotal role in both energy metabolism and recycling of the main excitatory neurotransmitter (Karaca et al., 2011), with potential impact on peripheral tissues.

Initial insights into CnsGlud1$^{-/-}$ mice showed that the lack of GDH in the CNS modified the metabolic handling of glutamate without altering synaptic transmission under basal conditions (Frigerio et al., 2012). In the present study, we investigated the metabolic role of brain GDH and the importance of glutamate as an energy substrate for the CNS. We first observed that control astrocytes could produce ATP in response to glutamate stimulation, following a first transient drop contributed by the energy-consuming uptake process (McKenna, 2013). While their glucose response was preserved, GDH null astrocytes isolated from CnsGlud1$^{-/-}$ mice were unable to generate ATP upon glutamate exposure, resulting in continuous and non-compensated ATP consumption. Accordingly, glutamate failed to activate mitochondria isolated from GDH null brains, whereas the GDH-independent substrate succinate efficiently induced mitochondrial respiration. These data demonstrate that astrocytes

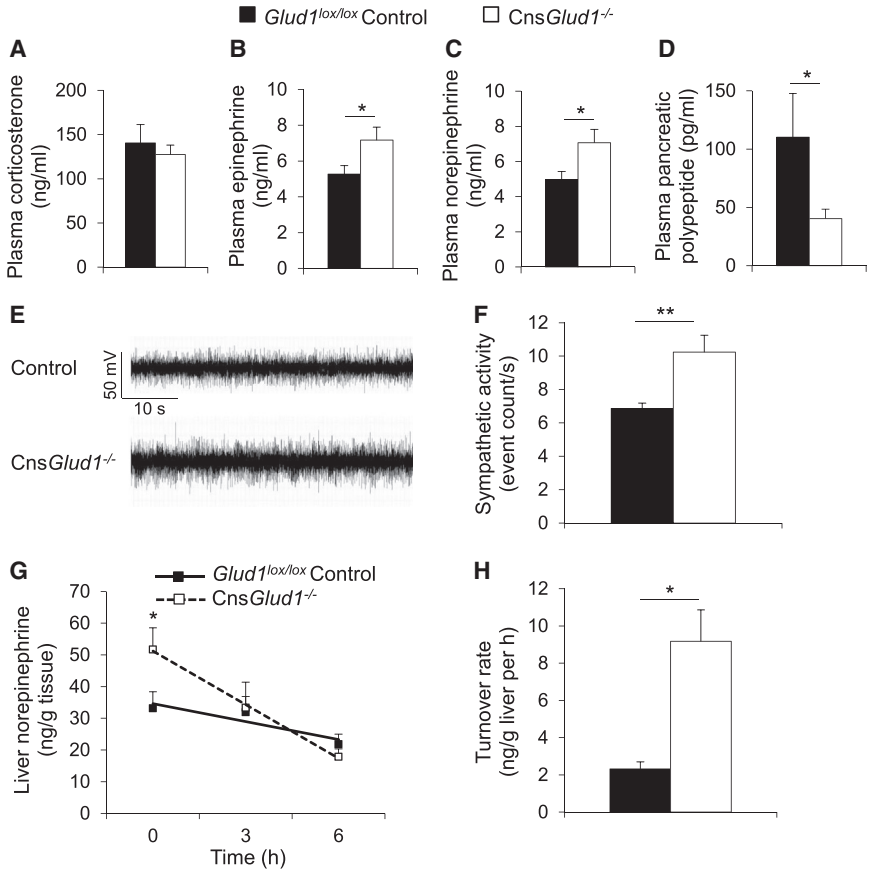

I

	Liver	
	Control	CnsGlud1-/-
NE_0 (ng.g^{-1})	29.9 ± 5.4	52.5 ± 9.5 *
k (h^{-1})	0.070	0.177
TR (ng.g^{-1}.h^{-1})	2.31 ± 0.38	9.17 ± 1.69 *

Figure 7. Increased Sympathetic and Decreased Parasympathetic Activities in CnsGlud1$^{-/-}$ Mice

(A–D) Plasma concentrations of corticosterone measured in the late light phase (A), epinephrine (B) and norepinephrine measured in fasting state (C), and pancreatic polypeptide measured in fed state (D) in Glud1$^{lox/lox}$ control and CnsGlud1$^{-/-}$ mice (n = 10–16).

(E–I) Sympathetic nervous system activity with representative recordings of sympathetic activity in Glud1$^{lox/lox}$ control and CnsGlud1$^{-/-}$ mice in the basal fed state (E) and quantification of sympathetic firing activity (F) (n = 7–8). Liver norepinephrine content (G) and turnover rate (H) after α-MPT injection. (I) Basal liver norepinephrine (NE) levels (NE_0), fractional turnover constants (k), and turnover rates (TR) (n = 4–6).

All values are means ± SEM. *p < 0.05; **p < 0.01.

can efficiently use glutamate for ATP production and that this process requires GDH. This energy-producing activity was abrogated in the absence of GDH, showing that transaminases do not compensate for the lack of GDH-dependent glutamate oxidation.

Lack of GDH-dependent glutamate oxidation resulted in increased hypothalamic ADP/ATP ratio and induced P-AMPK, a cellular energy sensor (Hardie and Carling, 1997). Both uptake and utilization of glucose were higher in CnsGlud1$^{-/-}$ brains compared to controls. Accordingly, lower brain glucose concentrations, remaining within the physiological range (Choi et al., 2001), were measured in CnsGlud1$^{-/-}$ brains along with peripheral normoglycemia. Astrocytes from CnsGlud1$^{-/-}$ mice efficiently generated ATP upon glucose stimulation, exhibiting even compensatory glucose responses compared with controls. Our data show that the deletion of GDH in the CNS subtracted glutamate as a source of energy, inducing compensatory usage of glucose by the brain.

The modified brain energy homeostasis in CnsGlud1$^{-/-}$ mice did not impact on global energy exchanges in terms of food intake and calorie expenditure. However, body composition was reshaped with increased fat mass and decreased lean mass, without net changes in body weight. In the periphery, CnsGlud1$^{-/-}$ mice exhibited lower glycemia under fasting conditions and glucose intolerance following a glucose load. Altered pancreatic function did not contribute to impaired peripheral glucose homeostasis, as glucose-stimulated insulin secretion was preserved in CnsGlud1$^{-/-}$ animals. Hyperinsulinemic-euglycemic clamp studies showed that glucose availability in CnsGlud1$^{-/-}$ mice was increased by both higher liver gluconeogenesis and lower muscle glucose uptake. We also observed increased plasma levels of ketone bodies, an alternative energy source for the CNS under conditions such as scarcity. Upregulation of the hormone-sensitive lipase in adipose tissues favored recruitment of fatty acids necessary for hepatic ketogenesis. Moreover, CnsGlud1$^{-/-}$ mice presented partial depletion of circulating glucogenic and ketogenic amino acids. These findings suggest metabolic adaptation of CnsGlud1$^{-/-}$ mice, with increased fat and muscle turnover providing energy substrates for the brain through liver function.

Maintenance of energy substrate homeostasis is crucial for the CNS and relies mainly on glucose provision from the periphery but also on recycled glutamate, as shown in the present study. The liver is the major source of glucose production. Hepatic glycogenolysis and gluconeogenesis promote glucose release into the bloodstream and availability for glucose-dependent tissues. In mammalian organisms, one of the most alarming states is a lowering of brain-compatible energy substrates, which induces counter-regulatory elevation of the sympathetic tone and in turn increases circulating levels of energy-recruiting hormones such as glucagon, adrenaline, and cortisol.

There are different mechanisms for CNS-mediated hormonal regulation of hepatic glucose production; among them, central AMPK plays a major role. Hypothalamic AMPK has been implicated in the regulation of food intake (Andersson et al., 2004; Kim et al., 2004a, 2004b; Lee et al., 2005; Minokoshi et al., 2004) and is activated in response to fasting or central glucoprivation (Kim et al., 2004b; Lee et al., 2005; Minokoshi et al., 2004). Stimulation of AMPK in the ventral hypothalamus increases endogenous glucose production (McCrimmon et al., 2004), whereas the latter is suppressed by inhibition of hypothalamic AMPK (Stoppa et al., 2008; Yang et al., 2010). AMPK participates in hypoglycemia sensing by promoting the release of counter-regulatory hormones such as adrenaline and glucagon, stimulating hepatic glucose production (McCrimmon et al., 2008). This is consistent with the reported stimulation of adrenal sympathetic nerve activity upon intracerebroventricular injection of AMPK activator (Tanida and Yamamoto, 2011).

Cns*Glud1*$^{-/-}$ mice exhibited increased hypothalamic P-AMPK levels in conditions of normoglycemia and elevated circulating catecholamines without changes in glucagon or corticosterone. Catecholamines are known to stimulate hepatic glucose production mainly through gluconeogenesis by promoting fuel mobilization. Cns*Glud1*$^{-/-}$ mice exhibited higher sympathetic tone, as revealed by the increased firing rates of the sympathetic nerve. In particular, the sympathetic outflow to the liver, as measured by catecholamine turnover, was increased in Cns*Glud1*$^{-/-}$ mice. Moreover, lower pancreatic polypeptide levels indicated that the parasympathetic outflow was lower in Cns*Glud1*$^{-/-}$ mice. Collectively, these results show that a change in the balance of the autonomous nervous system was instrumental in the phenotypic response of genetically suppressed brain GDH.

Regulation of hepatic glucose production via the SNS is mainly controlled by two mechanisms: neuronal stimulation of the neuroendocrine system, such as the release of adrenaline and glucagon, and direct liver innervation controlling glycogen metabolism (Shimazu, 1987). Vagal activation decreases blood glucose levels by inhibiting hepatic enzymes involved in gluconeogenesis and by activating those promoting glycogen synthesis (Shimazu, 1971), effects abolished by vagotomy (German et al., 2009; Matsuhisa et al., 2000). Recently, it was shown that activation of hypothalamic AMPK stimulates the SNS, which in turn activates hepatic gluconeogenesis and glycogenolysis via the stimulation of β-adrenergic receptors (Ikegami et al., 2013). It has also been proposed that the effects of hypothalamic AMPK on endogenous glucose production are mediated by neurons located at the dorsal vagal complex (Lam et al., 2010).

Based on our experimental data and the literature, we propose that a lack of GDH in CNS results in central energy scarcity translated into AMPK activation in the hypothalamus. This in turn activates the SNS and inhibits the parasympathetic nervous system. As a consequence, catecholamines may promote liver gluconeogenesis. Cns*Glud1*$^{-/-}$ mice exhibit moderate hypoglycemia in fasting conditions despite increased endogenous glucose production. The competing higher brain glucose uptake observed in knockout mice might contribute to this. Hypoglycemia-induced parasympathetic activity is known to stimulate glucagon secretion (Berthoud et al., 1990; Patel, 1984). Parasympathetic activity triggers the initial counter-regulatory response to temper hypoglycemia, whereas at lower glycemic levels, activation of sympathetic activity is induced (Taborsky and Mundinger, 2012). The lower parasympathetic tone of Cns*Glud1*$^{-/-}$ mice could explain their modest glucagon response to fasting conditions.

Overall, we observed that ablation of GDH in the CNS impaired oxidative metabolism of glutamate and increased brain glucose consumption. Cns*Glud1*$^{-/-}$ mice exhibited fasting-like brain energy sensor activation, despite normoglycemia, resulting in mobilization of energy substrates from the periphery through changes in the autonomous nervous system balance. This possible sequence of events will require further work to delineate the proposed roles for glutamate oxidation in CNS and related peripheral energy metabolism. The "energy-on-request" mechanisms illustrate here to which extent the brain dictates the partitioning of energy resources, in accordance with the "selfish brain" paradigm (Peters et al., 2004). Besides its paramount importance as a neurotransmitter, our study demonstrates that glutamate is an important energy substrate for the brain. It also highlights the key role of brain GDH in this process and in the fine-tuning of glutamate versus glucose utilization to maintain energy homeostasis. Altogether, our results show that GDH participates in central energy provision, modulating peripheral energy substrate partitioning.

EXPERIMENTAL PROCEDURES

Mice

Cns*Glud1*$^{-/-}$ mice, were generated as previously described (Frigerio et al., 2012). Animals were maintained on a mixed (C57BL/6J × 129/Sv) genetic background to avoid inbred strain-specific phenotypes. As control mice, we used *Glud1*$^{lox/lox}$ (*Glud1*$^{tm1.1Pma}$, MGI:3835667) littermates in order to optimize standardization of the genetic background between the two groups. To rule out the possibility that the Nestin-*Cre* transgene used in the present study may have independently contributed to the metabolic phenotype, we studied in parallel cohorts of mice carrying the Nestin-*Cre* transgene without floxed *Glud1* and wild-type littermates (Karaca and Maechler, 2014) to investigate some key metabolic parameters, revealing no effects of Nestin-*Cre* per se. Since no gender differences were noticed, data presented here are from males aged 11–13 weeks. Mice were maintained in our certified animal facility according to procedures that were approved by the animal care and experimentation authorities of the Canton of Geneva.

In Vivo Experiments

Brain metabolites were measured by NMR (^{1}H-MRS). Brain glucose uptake was evaluated following peripheral administration of [^{14}C]-2-deoxyglucose (Hartmann Analytic). Energy balance and body composition were assessed using metabolic cages and EchoMRI. Glucose and pyruvate tolerance tests were performed upon intraperitoneal injection of D-glucose (1 g/kg) or sodium pyruvate (2 g/kg) (Sigma-Aldrich) after an overnight fast. Insulin secretion was tested by in situ pancreatic perfusion and glucose turnover rate by hyperinsulinemic-euglycemic clamp. The firing rates of the SNS were measured during nerve recording experiments. The synthesis inhibition method of Brodie et al. was used to measure the catecholamines turnover rate (Brodie et al., 1966). Detailed procedures are given in Supplemental Experimental Procedures.

Determination of Metabolic Parameters

Oxygen consumption was measured on mitochondria isolated from brain and liver. Blood parameters were determined on samples collected from fed or overnight-fasting animals. Specific measurements are described in detail in Supplemental Experimental Procedures.

Please cite this article in press as: Karaca et al., GDH-Dependent Glutamate Oxidation in the Brain Dictates Peripheral Energy Substrate Distribution, Cell Reports (2015), http://dx.doi.org/10.1016/j.celrep.2015.09.003

Experiments on Isolated Astrocytes

Primary cultures of astrocytes were prepared from 7-day-old mice as described previously (Frigerio et al., 2012). Cellular ATP levels were measured in astrocytes transduced either with AdCAG-Luc adenovirus expressing the ATP-sensitive fluorescent probe luciferase or with ATeam adenovirus expressing the fluorescence resonance energy transfer (FRET)-based ATP indicator. The ^{13}C-labeling pattern in glutamate from incubation with [U-^{13}C]glucose was analyzed using gas chromatography mass spectrometry and the total amount of glutamate by high-performance liquid chromatography. Detailed protocols are given in Supplemental Experimental Procedures.

Expression Analyses by qRT-PCR, Immunoblotting, and Immunohistochemistry

Quantitative RT-PCR was performed on total RNA extracts. Antibodies against phospho-AMPKα (Thr172) (2531, Cell Signaling) and AMPKα (2532, Cell Signaling), were used for immunoblotting experiments on whole hypothalamus extracts. For immunohistochemistry, paraffin sections were stained using antibodies against insulin (I2018, Sigma-Aldrich) and glucagon (G2654, Sigma-Aldrich). Detailed protocols are described in Supplemental Experimental Procedures.

Statistics

Data are presented as means ± SEM. Statistical analyses were performed, using GraphPad Prism 6 software, with one-way ANOVA when more than two groups of data were compared, with two-way ANOVA when two conditions were involved, and with Student's t test when only two groups of data were concerned. We deemed the difference to be statistically significant when $p < 0.05$.

SUPPLEMENTAL INFORMATION

Supplemental information includes Supplemental Experimental Procedures and four figures and can be found with this article online at http://dx.doi.org/10.1016/j.celrep.2015.09.003.

AUTHOR CONTRIBUTIONS

M.K., F.F., S.M., J.M.-L., D.M.S., K.P., R.M.-R., and C.M. performed experiments. M.K., F.F., R.G., J.T.-R., H.S.W., C.M., and P.M. designed experiments, analyzed data, and wrote the paper.

ACKNOWLEDGMENTS

This work was supported by the State of Geneva, the Swiss National Science Foundation (310030B_135704 and 31003A_146984 to P.M.), the Synapsis Foundation (to P.M.), the Danish Medical Research Council (09-063399 to D.M.S. and 09-066319 to K.P.), and the Lundbeck (R77-A6808) and Carlsberg Foundations.

We are grateful to Dr. Y. Emre for helpful comments and Dr. N. Li for developing the ATP probe. We thank G. Chaffard, C. Vesin, F. Visentin, and H.M. Nielsen for expert technical assistance. We thank Drs. C. Poitry-Yamate and C. Cudalbu for NMR analyses.

Received: August 21, 2014
Revised: August 17, 2015
Accepted: September 1, 2015
Published: October 1, 2015

REFERENCES

Andersson, U., Filipsson, K., Abbott, C.R., Woods, A., Smith, K., Bloom, S.R., Carling, D., and Small, C.J. (2004). AMP-activated protein kinase plays a role in the control of food intake. J. Biol. Chem. *279*, 12005–12008.

Bak, L.K., Schousboe, A., and Waagepetersen, H.S. (2006). The glutamate/GABA-glutamine cycle: aspects of transport, neurotransmitter homeostasis and ammonia transfer. J. Neurochem. *98*, 641–653.

Baudry, M., and Lynch, G. (1979). Regulation of glutamate receptors by cations. Nature *282*, 748–750.

Berthoud, H.R., Fox, E.A., and Powley, T.L. (1990). Localization of vagal preganglionics that stimulate insulin and glucagon secretion. Am. J. Physiol. *258*, R160–R168.

Blouet, C., and Schwartz, G.J. (2010). Hypothalamic nutrient sensing in the control of energy homeostasis. Behav. Brain Res. *209*, 1–12.

Brodie, B.B., Costa, E., Dlabac, A., Neff, N.H., and Smookler, H.H. (1966). Application of steady state kinetics to the estimation of synthesis rate and turnover time of tissue catecholamines. J. Pharmacol. Exp. Ther. *154*, 493–498.

Choi, I.Y., Lee, S.P., Kim, S.G., and Gruetter, R. (2001). In vivo measurements of brain glucose transport using the reversible Michaelis-Menten model and simultaneous measurements of cerebral blood flow changes during hypoglycemia. J. Cereb. Blood Flow Metab. *21*, 653–663.

Danbolt, N.C. (2001). Glutamate uptake. Prog. Neurobiol. *65*, 1–105.

Escartin, C., Valette, J., Lebon, V., and Bonvento, G. (2006). Neuron-astrocyte interactions in the regulation of brain energy metabolism: a focus on NMR spectroscopy. J. Neurochem. *99*, 393–401.

Frigerio, F., Karaca, M., De Roo, M., Mlynárik, V., Skytt, D.M., Carobbio, S., Pajęcka, K., Waagepetersen, H.S., Gruetter, R., Muller, D., and Maechler, P. (2012). Deletion of glutamate dehydrogenase 1 (Glud1) in the central nervous system affects glutamate handling without altering synaptic transmission. J. Neurochem. *123*, 342–348.

Gaisler-Salomon, I., Miller, G.M., Chuhma, N., Lee, S., Zhang, H., Ghoddoussi, F., Lewandowski, N., Fairhurst, S., Wang, Y., Conjard-Duplany, A., et al. (2009). Glutaminase-deficient mice display hippocampal hypoactivity, insensitivity to pro-psychotic drugs and potentiated latent inhibition: relevance to schizophrenia. Neuropsychopharmacology *34*, 2305–2322.

German, J., Kim, F., Schwartz, G.J., Havel, P.J., Rhodes, C.J., Schwartz, M.W., and Morton, G.J. (2009). Hypothalamic leptin signaling regulates hepatic insulin sensitivity via a neurocircuit involving the vagus nerve. Endocrinology *150*, 4502–4511.

Gordon, J.A. (2010). Testing the glutamate hypothesis of schizophrenia. Nat. Neurosci. *13*, 2–4.

Gruetter, R., Novotny, E.J., Boulware, S.D., Mason, G.F., Rothman, D.L., Shulman, G.I., Prichard, J.W., and Shulman, R.G. (1994). Localized 13C NMR spectroscopy in the human brain of amino acid labeling from D-[1-13C] glucose. J. Neurochem. *63*, 1377–1385.

Hardie, D.G., and Carling, D. (1997). The AMP-activated protein kinase–fuel gauge of the mammalian cell? Eur. J. Biochem. *246*, 259–273.

Harris, L.W., Lockstone, H.E., Khaitovich, P., Weickert, C.S., Webster, M.J., and Bahn, S. (2009). Gene expression in the prefrontal cortex during adolescence: implications for the onset of schizophrenia. BMC Med. Genomics *2*, 28.

Hertz, L., Peng, L., and Dienel, G.A. (2007). Energy metabolism in astrocytes: high rate of oxidative metabolism and spatiotemporal dependence on glycolysis/glycogenolysis. J. Cereb. Blood Flow Metab. *27*, 219–249.

Hucho, F., Rasched, I., and Sund, H. (1975). Studies of glutamate dehydrogenase: analysis of functional areas and functional groups. Eur. J. Biochem. *52*, 221–230.

Ikegami, M., Ikeda, H., Ohashi, T., Ohsawa, M., Ishikawa, Y., Kai, M., Kamei, A., and Kamei, J. (2013). Olanzapine increases hepatic glucose production through the activation of hypothalamic adenosine 5′-monophosphate-activated protein kinase. Diabetes Obes. Metab. *15*, 1128–1135.

Karaca, M., and Maechler, P. (2014). Development of mice with brain-specific deletion of floxed glud1 (glutamate dehydrogenase 1) using cre recombinase driven by the nestin promoter. Neurochem. Res. *39*, 456–459.

Karaca, M., Frigerio, F., and Maechler, P. (2011). From pancreatic islets to central nervous system, the importance of glutamate dehydrogenase for the control of energy homeostasis. Neurochem. Int. *59*, 510–517.

Karnani, M., and Burdakov, D. (2011). Multiple hypothalamic circuits sense and regulate glucose levels. Am. J. Physiol. Regul. Integr. Comp. Physiol. *300*, R47–R55.

Kety, S.S. (1957). The general metabolism of the brain in vivo. In Metabolism of the Nervous System, D. Richter, ed. (Pergamon), pp. 221–237.

Kim, E.K., Miller, I., Aja, S., Landree, L.E., Pinn, M., McFadden, J., Kuhajda, F.P., Moran, T.H., and Ronnett, G.V. (2004a). C75, a fatty acid synthase inhibitor, reduces food intake via hypothalamic AMP-activated protein kinase. J. Biol. Chem. *279*, 19970–19976.

Kim, M.S., Park, J.Y., Namkoong, C., Jang, P.G., Ryu, J.W., Song, H.S., Yun, J.Y., Namgoong, I.S., Ha, J., Park, I.S., et al. (2004b). Anti-obesity effects of alpha-lipoic acid mediated by suppression of hypothalamic AMP-activated protein kinase. Nat. Med. *10*, 727–733.

Lam, C.K., Chari, M., and Lam, T.K. (2009). CNS regulation of glucose homeostasis. Physiology (Bethesda) *24*, 159–170.

Lam, C.K., Chari, M., Su, B.B., Cheung, G.W., Kokorovic, A., Yang, C.S., Wang, P.Y., Lai, T.Y., and Lam, T.K. (2010). Activation of N-methyl-D-aspartate (NMDA) receptors in the dorsal vagal complex lowers glucose production. J. Biol. Chem. *285*, 21913–21921.

Lee, K., Li, B., Xi, X., Suh, Y., and Martin, R.J. (2005). Role of neuronal energy status in the regulation of adenosine 5′-monophosphate-activated protein kinase, orexigenic neuropeptides expression, and feeding behavior. Endocrinology *146*, 3–10.

Lovatt, D., Sonnewald, U., Waagepetersen, H.S., Schousboe, A., He, W., Lin, J.H., Han, X., Takano, T., Wang, S., Sim, F.J., et al. (2007). The transcriptome and metabolic gene signature of protoplasmic astrocytes in the adult murine cortex. J. Neurosci. *27*, 12255–12266.

Magistretti, P.J., Pellerin, L., Rothman, D.L., and Shulman, R.G. (1999). Energy on demand. Science *283*, 496–497.

Mason, G.F., Gruetter, R., Rothman, D.L., Behar, K.L., Shulman, R.G., and Novotny, E.J. (1995). Simultaneous determination of the rates of the TCA cycle, glucose utilization, alpha-ketoglutarate/glutamate exchange, and glutamine synthesis in human brain by NMR. J. Cereb. Blood Flow Metab. *15*, 12–25.

Mastorodemos, V., Zaganas, I., Spanaki, C., Bessa, M., and Plaitakis, A. (2005). Molecular basis of human glutamate dehydrogenase regulation under changing energy demands. J. Neurosci. Res. *79*, 65–73.

Matsuhisa, M., Yamasaki, Y., Shiba, Y., Nakahara, I., Kuroda, A., Tomita, T., Iida, M., Ikeda, M., Kajimoto, Y., Kubota, M., and Hori, M. (2000). Important role of the hepatic vagus nerve in glucose uptake and production by the liver. Metabolism *49*, 11–16.

McCrimmon, R.J., Fan, X., Ding, Y., Zhu, W., Jacob, R.J., and Sherwin, R.S. (2004). Potential role for AMP-activated protein kinase in hypoglycemia sensing in the ventromedial hypothalamus. Diabetes *53*, 1953–1958.

McCrimmon, R.J., Shaw, M., Fan, X., Cheng, H., Ding, Y., Vella, M.C., Zhou, L., McNay, E.C., and Sherwin, R.S. (2008). Key role for AMP-activated protein kinase in the ventromedial hypothalamus in regulating counterregulatory hormone responses to acute hypoglycemia. Diabetes *57*, 444–450.

McKenna, M.C. (2007). The glutamate-glutamine cycle is not stoichiometric: fates of glutamate in brain. J. Neurosci. Res. *85*, 3347–3358.

McKenna, M.C. (2012). Substrate competition studies demonstrate oxidative metabolism of glucose, glutamate, glutamine, lactate and 3-hydroxybutyrate in cortical astrocytes from rat brain. Neurochem. Res. *37*, 2613–2626.

McKenna, M.C. (2013). Glutamate pays its own way in astrocytes. Front. Endocrinol. (Lausanne) *4*, 191.

McKenna, M.C., Sonnewald, U., Huang, X., Stevenson, J., and Zielke, H.R. (1996). Exogenous glutamate concentration regulates the metabolic fate of glutamate in astrocytes. J. Neurochem. *66*, 386–393.

Meldrum, B.S. (1994). The role of glutamate in epilepsy and other CNS disorders. Neurology *44* (*11, Suppl 8*), S14–S23.

Michaelidis, T.M., Tzimagiorgis, G., Moschonas, N.K., and Papamatheakis, J. (1993). The human glutamate dehydrogenase gene family: gene organization and structural characterization. Genomics *16*, 150–160.

Minokoshi, Y., Alquier, T., Furukawa, N., Kim, Y.B., Lee, A., Xue, B., Mu, J., Foufelle, F., Ferré, P., Birnbaum, M.J., et al. (2004). AMP-kinase regulates food intake by responding to hormonal and nutrient signals in the hypothalamus. Nature *428*, 569–574.

Nehlig, A. (2004). Brain uptake and metabolism of ketone bodies in animal models. Prostaglandins Leukot. Essent. Fatty Acids *70*, 265–275.

Patel, D.G. (1984). Role of parasympathetic nervous system in glucagon response to insulin-induced hypoglycemia in normal and diabetic rats. Metabolism *33*, 1123–1127.

Peters, A., Schweiger, U., Pellerin, L., Hubold, C., Oltmanns, K.M., Conrad, M., Schultes, B., Born, J., and Fehm, H.L. (2004). The selfish brain: competition for energy resources. Neurosci. Biobehav. Rev. *28*, 143–180.

Rolfe, D.F., and Brown, G.C. (1997). Cellular energy utilization and molecular origin of standard metabolic rate in mammals. Physiol. Rev. *77*, 731–758.

Sanner, T. (1975). Formation of transient complexes in the glutamate dehydrogenase catalyzed reaction. Biochemistry *14*, 5094–5098.

Shimazu, T. (1971). Regulation of glycogen metabolism in liver by the autonomic nervous system. V. Activation of glycogen synthetase by vagal stimulation. Biochim. Biophys. Acta *252*, 28–38.

Shimazu, T. (1987). Neuronal regulation of hepatic glucose metabolism in mammals. Diabetes Metab. Rev. *3*, 185–206.

Sokoloff, L. (1960). Metabolism of the central nervous system in vivo. In Handbook of Physiology: Neurophysiology, J. Field, H.W. Magoun, and V.E. Hall, eds. (American Physiological Society), pp. 1843–1864.

Stoppa, G.R., Cesquini, M., Roman, E.A., Prada, P.O., Torsoni, A.S., Romanatto, T., Saad, M.J., Velloso, L.A., and Torsoni, M.A. (2008). Intracerebroventricular injection of citrate inhibits hypothalamic AMPK and modulates feeding behavior and peripheral insulin signaling. J. Endocrinol. *198*, 157–168.

Taborsky, G.J., Jr., and Mundinger, T.O. (2012). Minireview: The role of the autonomic nervous system in mediating the glucagon response to hypoglycemia. Endocrinology *153*, 1055–1062.

Tanida, M., and Yamamoto, N. (2011). Central AMP-activated protein kinase affects sympathetic nerve activity in rats. Neurosci. Lett. *503*, 167–170.

Vannucci, S.J., Maher, F., and Simpson, I.A. (1997). Glucose transporter proteins in brain: delivery of glucose to neurons and glia. Glia *21*, 2–21.

Verleysdonk, S., and Hamprecht, B. (2000). Synthesis and release of L-serine by rat astroglia-rich primary cultures. Glia *30*, 19–26.

Westergaard, N., Drejer, J., Schousboe, A., and Sonnewald, U. (1996). Evaluation of the importance of transamination versus deamination in astrocytic metabolism of [U-13C]glutamate. Glia *17*, 160–168.

Yang, X.J., Kow, L.M., Pfaff, D.W., and Mobbs, C.V. (2004). Metabolic pathways that mediate inhibition of hypothalamic neurons by glucose. Diabetes *53*, 67–73.

Yang, C.S., Lam, C.K., Chari, M., Cheung, G.W., Kokorovic, A., Gao, S., Leclerc, I., Rutter, G.A., and Lam, T.K. (2010). Hypothalamic AMP-activated protein kinase regulates glucose production. Diabetes *59*, 2435–2443.

Yu, A.C., Schousboe, A., and Hertz, L. (1982). Metabolic fate of 14C-labeled glutamate in astrocytes in primary cultures. J. Neurochem. *39*, 954–960.

Zaganas, I., Waagepetersen, H.S., Georgopoulos, P., Sonnewald, U., Plaitakis, A., and Schousboe, A. (2001). Differential expression of glutamate dehydrogenase in cultured neurons and astrocytes from mouse cerebellum and cerebral cortex. J. Neurosci. Res. *66*, 909–913.

Zaganas, I., Spanaki, C., and Plaitakis, A. (2012). Expression of human GLUD2 glutamate dehydrogenase in human tissues: functional implications. Neurochem. Int. *61*, 455–462.

Zielke, H.R., Zielke, C.L., and Baab, P.J. (2009). Direct measurement of oxidative metabolism in the living brain by microdialysis: a review. J. Neurochem. *109* (*Suppl 1*), 24–29.